(Received 14 October 2024, Accepted 26 November 2024, Scheduled 25 December 2024)

A Compact, Conformal DRA with Integrated Feed for Low-Profile Applications

Pramod K. Gupta[1], Garima Tiwari[1], Manshree Mishra[1], and Biswajeet Mukherjee[2]

[1]*Department of Electronics & Communication, PDPM IIITDM Jabalpur, India*
[2]*Department of Electronic Science, University of Delhi, India*

ABSTRACT: A novel compact low-profile Conformal Dielectric Resonator Antenna (CDRA) for wideband applications is proposed. By employing a specially designed dielectric resonator in conjunction with an inverted-trapezoidal patch for feeding, an extensive Impedance Bandwidth (IB) around 51.5% is realized. The resonant frequencies of 6 GHz and 7.5 GHz correspond to the observation of the $TE_{21\delta}$ mode and the second higher-order $TE_{23\delta}$ mode, respectively. Moreover, a realized peak gain of 7.2 dBi is attained at 7.4 GHz. The proposed DRA offers a wide IB with more than 90% radiation efficiency throughout the bandwidth. Additionally, a good alignment is observed between the measured and simulated results. The proposed DRA is compact and has a low profile of $0.1\lambda_g$, where λ_g represents the wavelength at the lower cut-off frequency. A CDRA with a conformal feed is an innovative design tailored for wireless communication systems operating within the frequency range from 5.2 GHz to 8.8 GHz. This antenna configuration is specifically engineered to exhibit conformal properties, enabling it for applications such as the exteriors of vehicles, aircraft, or other non-planar structures.

1. INTRODUCTION

Dielectric resonator antennas (DRAs) have gained significant attention in recent years due to their promising characteristics, including high radiation efficiency, low profile, and suitability for various wireless communication applications. However, there are still several challenges and opportunities for improvement in the design and optimization of DRAs for next-generation wireless communication systems [1]. The swift evolution of modern communication applications drives the need for antennas with wider bandwidth, compact and low profile, high gain, and superior radiation efficiency to satisfy requirements arising to meet the escalating demands of wireless data users. Rectangular DRAs are commonly utilized due to their fabrication simplicity and greater design versatility than hemispherical or cylindrical configurations. Their structure supports low-profile applications, providing two degrees of design flexibility through optimized width-to-height and height-to-length ratios [2]. The DRA is frequently suggested as a superior alternative to the microstrip patch antenna; however, for a relevant comparison, the DRA must maintain a low profile. A low-profile rectangular DRA with a length-to-height ratio about six is described in [3]. Recent advancements in wireless communication systems have spurred the development of wideband and multiband antennas. To address the issue of bandwidth limitations, unconventional shapes of DRAs have been devised, including designs with air gaps such as U-shaped [4], T-shaped [5], A-shaped [6], and triangular [7] ones. However, in many instances, achieving a wide bandwidth has led to enlarged size of the antenna structure and intricate shapes.

Another method for enhancing bandwidth is to stack two dielectric materials with different dielectric constants on top of each other, as demonstrated in [8] and [9]. However, this approach frequently leads to increased bulkiness of the antenna. Fractal is another technique used to improve the impedance BW. The self-similar property of fractals plays a crucial role in optimizing the antenna's performance by facilitating the alignment of resonant modes, ultimately leading to a wider impedance bandwidth and improved versatility for wideband applications [10]. As fractal iteration increases, the surface-area to volume ratio in a Dielectric Resonator Antenna also increases. This augmentation leads to an improvement in the quality factor (Q-factor) and typically results in enhanced antenna impedance bandwidth [11]. A fractal DRA for WiMAX applications is introduced in [12], and Sierpinski and Minkowski, two fractal techniques, are combined in [13]. However, both structures are complex and exhibit limited bandwidths of 14% and 66%, respectively. Subsequently, various feeding techniques are employed in DRAs, including the use of conformal metal strips and trapezoidal-shaped feeding mechanisms [14, 15], which effectively enhance the impedance bandwidth.

The studies mentioned earlier all involve dielectric blocks with flat bottoms placed on a planar surface. For non-planar platforms, a conformal antenna is preferred due to its inherently low profile and compact size. This communication provides an extensive investigation of concave bent DRAs with conformal Ground Plane (GP). Initially, an approximate model provides the foundation for theoretical investigation [16, 17]. The eigenmode approach and single-mode approximation are then used in order to divide the resonant modes of a bent DRA into TE and TM to z-direction modes. In cylindrical coordinates,

* Corresponding author: Pramod Kumar Gupta (Pramod603gupta@gmail.com).

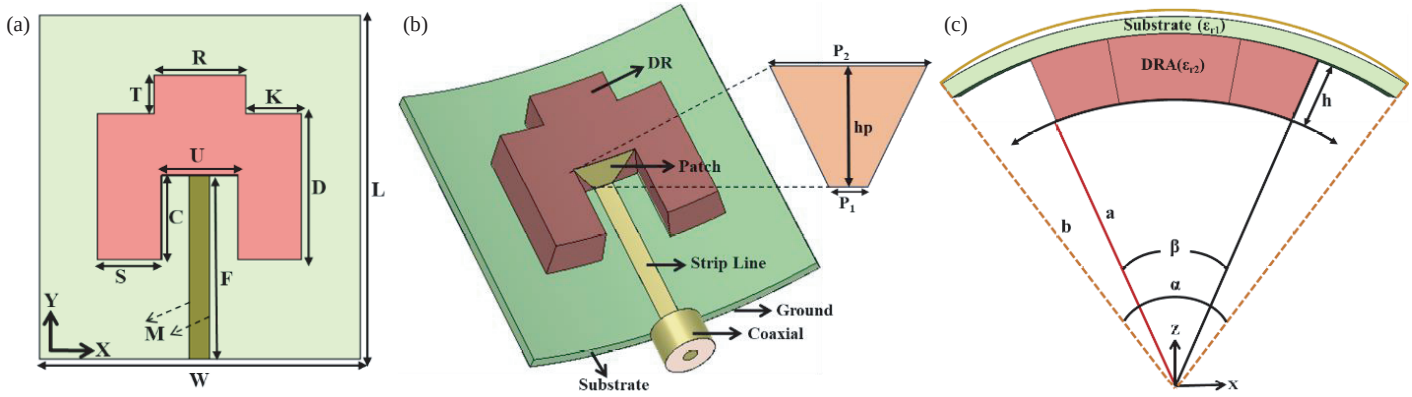

FIGURE 1. Proposed DRA geometry with relevant dimensions provided in the caption: (a) top view and (b) prospective view, (c) conformal view of the proposed DRA.

unlike in rectangular coordinates, only the z-directional components of the electromagnetic field can independently represent all other field components. Therefore, the fields in bent dielectric resonator antennas (DRAs) are classified into TEz and TMz modes. The TEz modes in bent DRAs are similar to those in rectangular DRAs (RDRAs), while the TMz modes in bent DRAs, which have no magnetic field along the z-axis, correspond to the TEx modes in RDRAs [19–21]. In this paper, a compact, low-profile miniaturized arc Dielectric Resonator Antenna (DRA) with conformal feed structures is investigated. The term "low-profile" refers to minimizing the antenna's physical height relative to its operating wavelength.

2. CONFORMAL DRA DESIGN AND ANALYSIS

The resonant frequency of the dielectric resonator is defined by its dimensions and the dielectric constant of the material. By exploiting this resonance phenomenon, Conformal DRAs can achieve efficient radiation characteristics suitable for various wireless communication and sensing applications. Theoretical models describing the electromagnetic behavior of dielectric resonators, including mode analysis and field distribution, provide insights into the design parameters influencing the antenna's performance.

The configuration of the proposed DRA is depicted in Fig. 1(a), where a symmetrical shape DR is placed at the center of the $42 \times 45\,\text{mm}^2$ substrate with a low permittivity of $\varepsilon_{r1} = 3.5$, and the underside of the substrate is coated with copper as the ground plane. A dielectric resonator (DR) in contact with the base substrate is constructed using Taconic RF-10, which possesses a relative dielectric constant of $\varepsilon_{r2} = 10.2$.

The DR is excited by an inverted-trapezoidal patch etched at the center of the DR. This patch is then connected to an SMA connector via a 50-ohm microstrip line. Conformal strip feeding is notably advantageous over probe feeding due to the absence of drilling requirements and the prevention of air gaps between the DR and the feed. Efficient energy coupling can be attained through conformal feeding [18]. The dimensions of the antenna are 42 mm along the X-axis and 45 mm along the Y-axis. The perspective illustration of the proposed Conformal DRA can be seen in Fig. 1(b). After conducting a parametric analysis of the proposed design using CST STUDIO SUITE, the optimal design parameters obtained are as follows: $L = 45\,\text{mm}$, $W = 42\,\text{mm}$, $R = 12\,\text{mm}$, $S = 8.25\,\text{mm}$, $T = 5\,\text{mm}$, $U = 10\,\text{mm}$, $D = 19\,\text{mm}$, $K = 7.25\,\text{mm}$, $M = 2.7\,\text{mm}$, $F = 24\,\text{mm}$, $C = 11\,\text{mm}$, $h = 5.5\,\text{mm}$. $P1 = 2.7\,\text{mm}$, $P2 = 10\,\text{mm}$, $hp = 5.5\,\text{mm}$. The proposed conformal DRA configuration is presented in Fig. 1(c). In this configuration, the DRA is placed on the conformal ground plane. Since the symmetrical ground plane is assumed, α and β are the angles of the conformal ground and conformal DR simultaneously where $\alpha = 40.5°$ and $\beta = 25.5°$ for the radius $R = 60\,\text{mm}$.

3. INVESTIGATION OF CONFORMAL GROUND PLANE

In this section, the impact of conformal ground effects on the radiation characteristics of an arc Dielectric Resonator Antenna (DRA) is investigated. The metallic ground plane is assumed to be arc shaped. The significance of the two fundamental modes of arc DRAs lies in their widespread popularity and interest [19]. The radiation mechanism of a planar and concave conformal DRA is demonstrated by the geometric theory of diffraction, as seen in Fig. 2. The perspective of electromagnetic fields theory provides a precise understanding of the impact of ground effect on radiation performance. For a plane surface, the edges are primarily responsible for the diffraction effect [20]. Due to the smooth convexity, surface diffraction also appears on arc-shaped ground in addition to edge diffraction, and the reflection dominates on concave ground plane [21]. Based on the semi-cavity model, the bent DRA in Fig. 1 is analysed. The sidewalls cannot be treated as perfect magnetic conductors (PMCs) due to the presence of hybrid modes [19]. Although PMC-based cavity and semi-cavity models are commonly used for analyzing triangular [22] and sectored [23] DRAs, these studies typically focus on flat ground planes. Research on conformal and flexible DRAs remains limited. The ground plane is considered as a Perfect Electrical Conductor (PEC). As a result, this approximate model does not take the substrate into account. However, image theory for conventional DRAs is no longer possible because a bent GP cannot be assumed to be an infinite PEC plane.

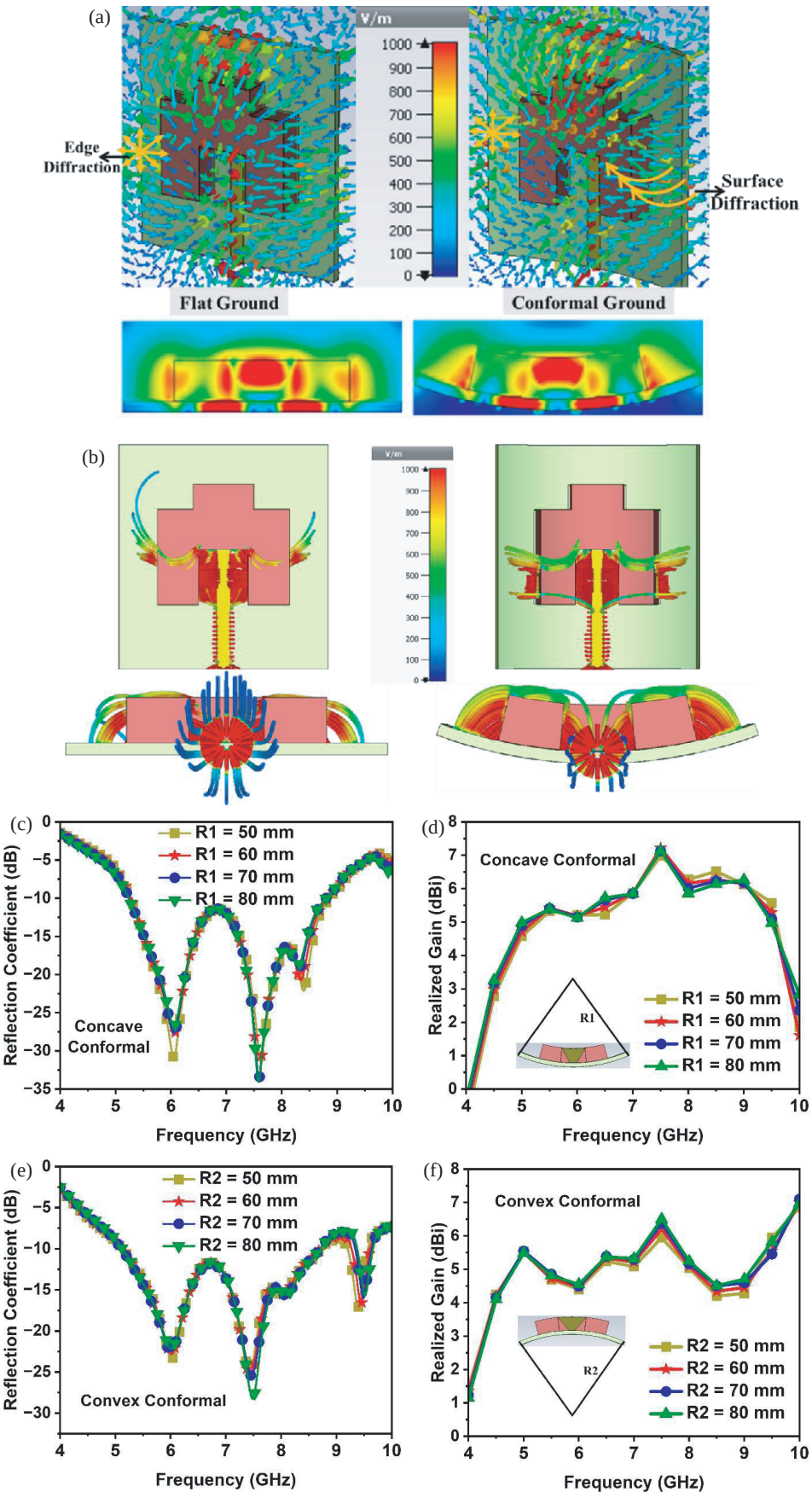

FIGURE 2. (a) Vector E-field distributions and scalar E-field distributions. (b) $Streamline$ E-field distributions of flat and conformal DRA, reflection coefficient, and gain variation for different ground plane radii $R1$ and $R2$: (c) Reflection coefficient — concave, (d) Gain — concave, (e) Reflection coefficient — convex, (f) Gain — convex.

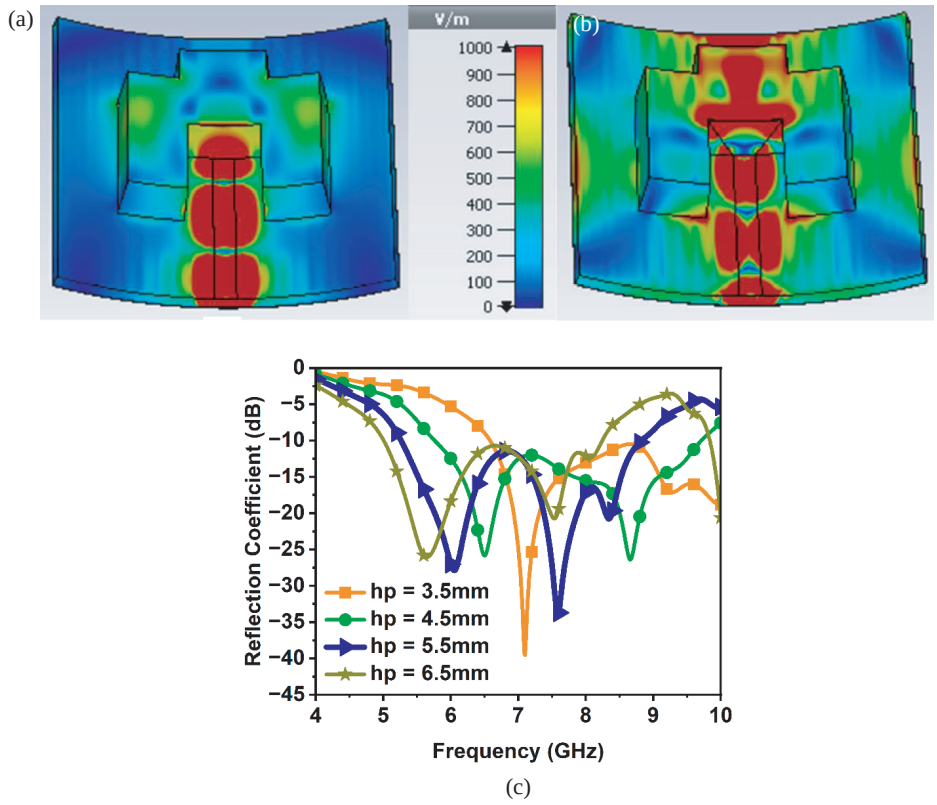

FIGURE 3. E-field distribution (a) without integrated patch, (b) with integrated patch, (c) reflection coefficient plot for the integrated trapezoidal patch height variation.

Hence, as compared to flat DRA, bend DRA lacks their usual isolated counterparts. In such cases, the bottom surface and side walls in α-direction are considered as PMCs [21]. In order for electromagnetic waves to travel outward and decrease exponentially, the infinitely large interfaces between two different dielectric media are intended to form lateral boundaries along the z-direction. A flat DRA undergoes concave conformal geometric processing to transform into a conformal DRA. The curvature angle of the proposed structure impacts the radiation patterns in both co-polarization and cross-polarization where gain, 3-dB angular beamwidth, and side lobe level (SLL) of the DRA are affected. At $\alpha = 40.5°$, higher gain is attained for co-polarization than other angles. Thus, it is chosen for the proposed antenna design. Moreover, at this specific value of α, both the 3 dB angular beamwidth and the SLL fall within acceptable ranges. On an arc ground, smooth concavity causes surface reflection and edge diffraction, while planar GP diffraction effects mainly occur due to edges, as illustrated in Fig. 2(a). The concave bending of the ground causes a more directional surface reflection, which leads to enhancement of the gain of the DRA. However, the surface reflection on the flat GP is less directional as shown in Fig. 2(a).

Streamlines are a powerful visualization technique used to depict the flow of electric field lines within the structure as shown in Fig. 2(b). Parametric behaviours can indeed be extended to convex platforms, although the antenna's performance may vary due to changes in the surface curvature that affect electromagnetic wave propagation and impedance characteristics. The behaviour of the reflection coefficient and gain for various radii of concave conformal ground planes are illustrated in Fig. 2(c) and Fig. 2(d), respectively. Similarly, Fig. 2(e) and Fig. 2(f) depict the reflection coefficient and gain behaviour for various radii of convex conformal ground planes. The plot shows that the reflection coefficient and gain remain nearly consistent across different curvature radii for both concave and convex conformal dielectric resonator antennas (DRAs). However, the concave conformal ground plane demonstrates superior performance compared to the convex configuration, making it the preferred choice for the conformal DRA design in this study. Future work will consider a comparative analysis to explore these behaviours in convex configurations, providing a broader understanding of the design adaptability across various surface geometries. Additionally, multiband antenna configurations could be investigated to support a wider range of applications in modern wireless communication. Optimizing material properties and feed mechanisms may enhance compatibility with 5G and internet of things (IoT), while further miniaturization and array configurations could enable beam-steering and improve directional control for autonomous systems and satellite communication.

3.1. Effect of Integrated Patch Loading

The characteristics of z-directional patch loading is discussed in this section. The E-field distribution is presented in Fig. 3(a)

without trapezoidal patch and in Fig. 3(b) with the trapezoidal patch.

The reflection coefficient plot for various heights of the integrated patch-loaded feed is illustrated in Fig. 3(c). The height of the DRA and conformal trapezoidal patch increases in the z-direction can significantly broaden the impedance bandwidth of the DRA. The plot indicates that as the patch height decreases, the reflection coefficient tends to shift towards higher frequencies. Conversely, when the patch height increases, there is an improvement in the matching between the integrated patch connected to the microstrip line and the DRA, leading to a shift of the reflection coefficient towards lower frequencies. Hence, the additional coupling introduced by the patch can improve impedance matching and enhance the antenna's bandwidth, allowing it to operate over a wider range of frequencies. The shape of the feeding patch is optimized to ensure good impedance matching in a wide frequency range. In order to foster conformal applications, the DRA height is maintained in low profile. The optimized height of the DRA is $0.1\lambda_g$ (5.5 mm).

4. DESIGN METHODOLOGY AND PARAMETRIC STUDY

The wideband characteristic and size miniaturization of the proposed DRA are realized through a multi-step design procedure, including selecting the dielectric material, determining the resonant frequency, designing the antenna structure, and optimizing its performance through parametric studies. Initially, for configuration-1, Dielectric Waveguide Model (DWM) is used to design a conventional rectangular DRA. In rectangular DRA, the following transcendental Equation (1) is used to determine the resonant frequency (f_0) for the fundamental $\mathrm{TE}^{x}_{11\delta}$ mode.

$$f_0 = \frac{C}{2\pi\sqrt{\varepsilon_r}}\sqrt{k_x^2+k_y^2+{k_z}^2} \tag{1}$$

$$\text{where : —} \quad \lambda k_0=\frac{2\pi}{0}=\frac{2\pi f_0}{c},\ k_x=\frac{\pi}{p},\ k_z=\frac{\pi}{r},$$

$$\text{and } k_x^2+k_y^2+{k_z}^2=\varepsilon_r k_0^2$$

In the aforementioned equations, ε_r represents the dielectric constant of the DR, k_0 denotes the free space wave number; c is the velocity of light; and kx, ky, and kz are the wave numbers along the x, y, and z directions, respectively.

The progression towards the development of the proposed antenna is illustrated in Fig. 4(a), and its corresponding bandwidth performance for each step is illustrated in Fig. 4(b). Configuration-1, composed of a homogenous rectangular shape dielectric resonator (DR), is created and excited by a simple microstrip line. In configuration-2, the optimized conformal trapezoidal microstrip feeding patch is introduced to ensure good impedance matching in a wide frequency range. In configuration-3, a rectangular notch is incorporated into the dielectric resonator (DR), resulting in an increase of the surface-area to volume (S/V) ratio. Following the principles of image theory, the notched portion resembles a rectangular "ring", and by modifying the dimensions of the length and width of the notch, the bandwidth is enhanced.

Finally, an optimized DRA with a conformal trapezoidal patch loaded feed is obtained as shown in configuration-4, which provides electrical length miniaturization and offers a wideband response of 3.6 GHz from 5.2 GHz to 8.8 GHz with an enhanced gain of the proposed DRA. Fig. 4(b) provides a comparison of the reflection coefficient for each DRA configuration, which clearly demonstrates that configuration-4 stands out as an optimized design. The reflection coefficient and realised gain for the flat and conformal ground plane are shown in Fig. 4(c) and Fig. 4(d). It can be observed that the bandwidth remains nearly the same but is slightly shifted towards the higher frequencies for the concave conformal ground, accompanied by an improvement in realized gain. This is because the surface reflection becomes more focused and narrows as the radius of the concave conformal ground plane decreases. A parametric study of some important parameters is performed to further analyze the proposed antenna, and its effect on reflection coefficient is observed. In each scenario, only one parameter is varied while the remaining ones are maintained constant. The simulated reflection coefficient characteristics for various values of C and T are shown in Figs. 4(e) and 4(f), respectively. The reflection coefficient decreases with a decrease in C and an increase in T. This occurs because a decrease in C and an increase in T enhance the electrical coupling between the transmission line and dielectric resonator (DR). Additionally, both C and T significantly impact the fundamental mode and higher-order modes. It can be observed from Fig. 4(e) that all values other than $C = 11$ mm provide many different bands with narrow bandwidth and poor impedance matching. Thus, the optimal value of C is fixed at 11 mm. Subsequently, further investigation is conducted to change the value of T. The plot of reflection coefficient variations for different values of T is shown in Fig. 4(f). The optimized value of T is fixed at 5 mm. For $T = 3$ mm, 4 mm, 6 mm, 7 mm, the impedance bandwidth is less than the optimized value.

4.1. Field Distribution and Mode Analysis

The simulated electric field distributions of the proposed DRAs at various frequencies and modes are depicted in Fig. 5(a) and Fig. 5(b). The first higher-order and second higher-order broadside modes of the proposed DRAs can be seen in this figure. The simulated field pattern indicates a continuous rotation of the electric field vectors within a constant azimuthal plane, spanning from 0° degrees to 360° degrees. The investigation of E-field variations in the proposed antenna reveals that it supports the $\mathrm{TE}_{22\delta}$ modes at 6 GHz and $\mathrm{TE}_{23\delta}$ mode at 7.5 GHz, respectively, which is concurrence with modes explained in [1, 2].

5. EXPERIMENTAL RESULTS AND DISCUSSION

The fabricated prototype of proposed conformal DRA and corresponding results is shown in Fig. 6(a)–Fig. (f). The conformal ground plane is accomplished by truncating a copper printed substrate of Taconic RF-35 dielectric sheet into a rectangle of $W \times L\,\mathrm{mm}^2$, achieved by Computerized Numerical Control (CNC) machine and then molding it around a mold of radius

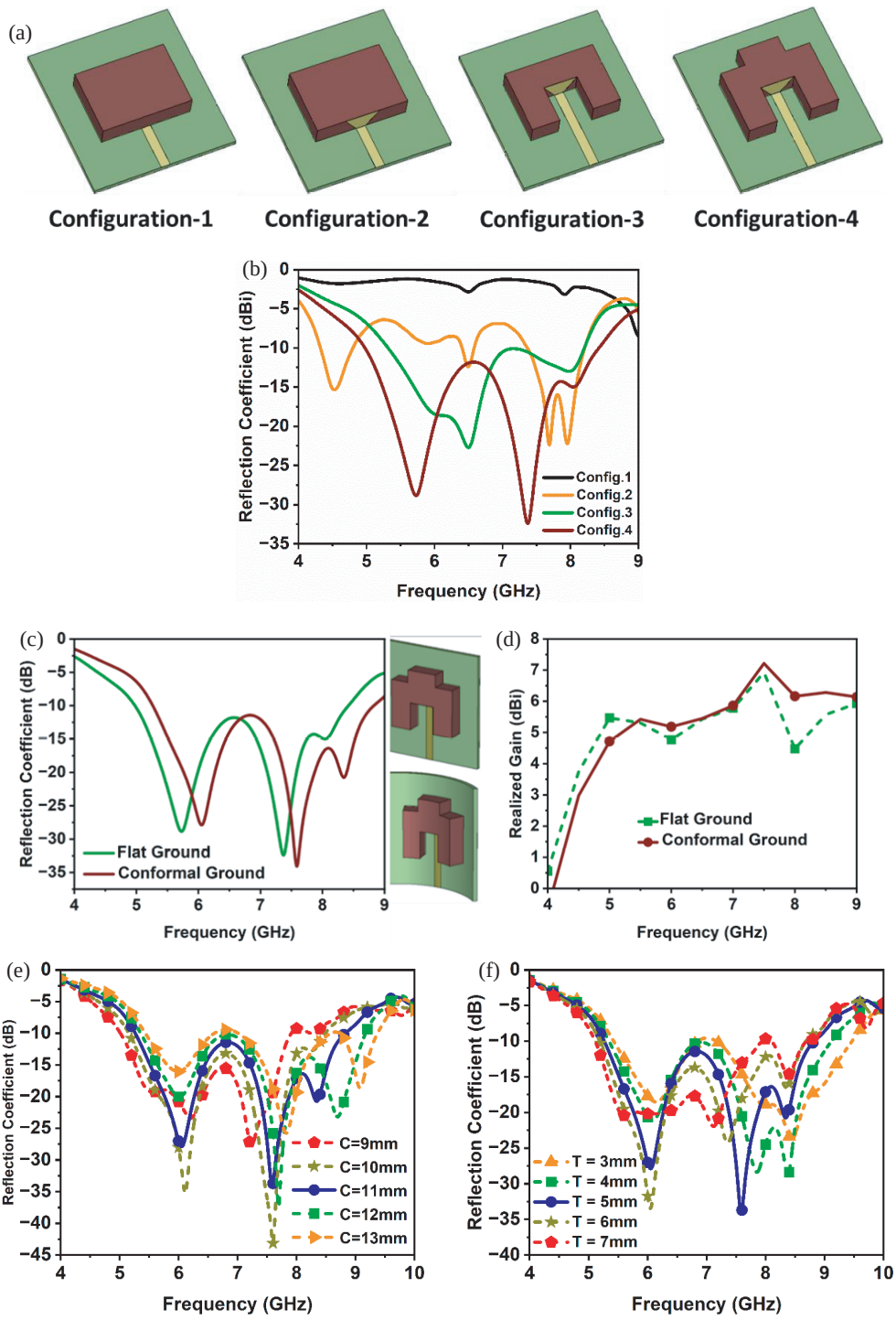

FIGURE 4. The progressive development stages of the proposed DRA. (a) Config. 1, Config. 2, Config. 3 and Config. 4. (b) Reflection coefficient plot for the different configurations — 1, 2, 3, and 4. Effect of flat and conformal ground on (c) Reflection coefficient and (d) Realised gain. Effect of changing the reflection coefficient plot for different parameter values. (e) Effect of C on reflection coefficient and (f) Effect of T on reflection coefficient for the proposed DRA.

60 mm. The DR is fabricated using 1.5 mm thick Taconic RF-10 material with a dielectric constant of 10.2 which is subjected to water jet machining. The individual layers are then stacked to obtain the optimised height of the proposed structure by using commercially available araldite glue applied at the edges under high pressure. This is done to avoid any deviation between simulated and measured results.

The prototypes of Conformal DRAs are fabricated and tested in an anechoic chamber. Measured results are compared with simulation data to assess the accuracy of the numerical models and identify any discrepancies.

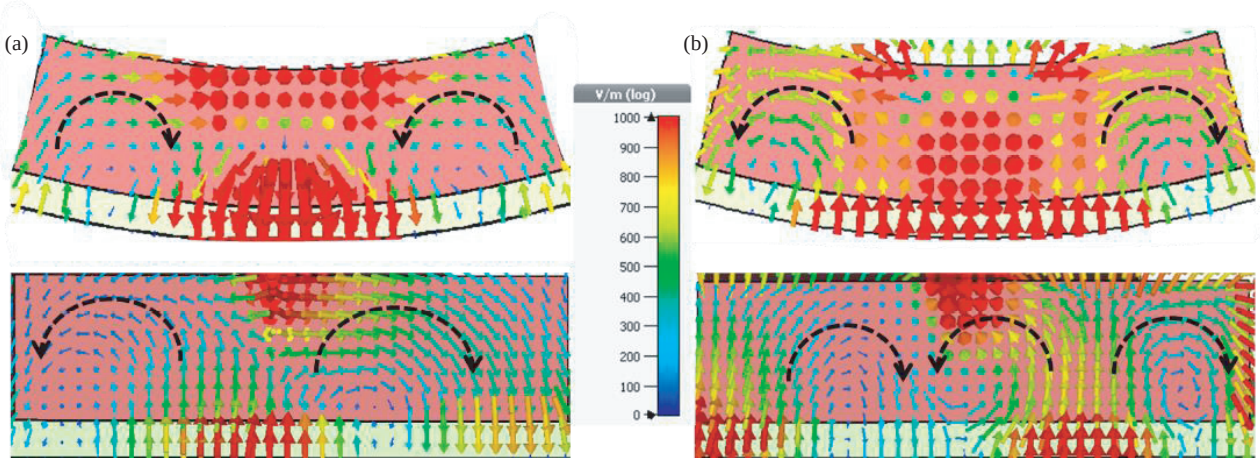

FIGURE 5. Simulated vector E-field distributions at (a) 5.8 GHz and (b) 7.5 GHz.

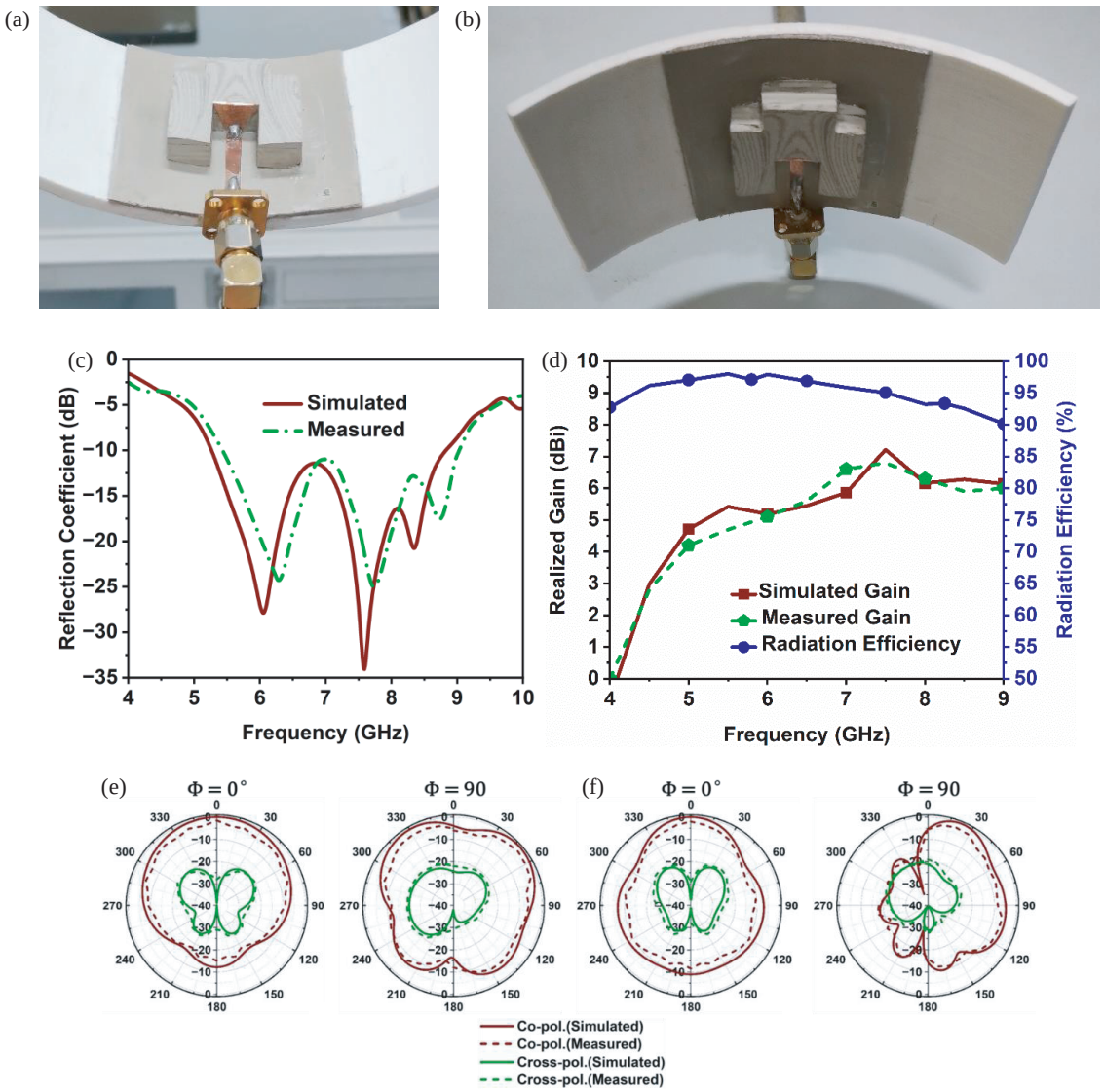

FIGURE 6. The fabricated prototype. (a) Top view. (b) Conformal view of proposed DRA. (c) Measured and simulated reflection coefficient. (d) Realized gain, simulated radiation efficiency, and radiation patterns of proposed DRA at $\Phi = 0°$ and $\Phi = 90°$. (e) 6 GHz. (f) 7.5 GHz.

TABLE 1. Comparison of proposed DRAs with existing literature.

Ref.	DRA Height (λg)	ε_r	IB (%)	Peak Gain (dBi)	Design Technique	Operating Frequencies (GHz)
[19]	0.09	9.9	18.4	7	CBDRA + AC	6.8 to 8.2
[20]	0.08	9.9	16.5	4	CDRA	5.8 to 6.9
[21]	0.08	12.3	14.2	7	SFADRA	2.3 to 2.7
[24]	0.31	10	22	6.5	RDRA + CPP	3.6 to 4.45
[25]	0.1	9	26	5	CSDRA	2 to 2.6
[26]	NA	NA	10.2	9	CMPA	5.15 to 5.68
[27]	NA	NA	33.5	2.62	CPA + CPW-Fed	2.01 to 2.82
P.W.	**0.1**	**10.2**	**51.5**	**7.2**	**CDRA + IF**	**5.2 to 8.8**

The simulated and measured reflection coefficients exhibit good agreement, as illustrated in Fig. 6(c). However, minor discrepancies arise due to fabrication tolerances, the positioning of the DRA on the ground plane, etc. The fabricated DRA resonates at two frequencies, 6 GHz and 7.5 GHz, providing a wideband range from 5.2 GHz to 8.8 GHz, with a percentage bandwidth about 51.5%. To measure the gain of the conformal DRA, the two-antenna method was employed, utilizing a broadband horn antenna as the transmitting antenna. The realized gain and simulated radiation efficiency of the proposed DRA are presented in Fig. 6(d). The measured peak gain is about 6.8 dBi at 7.5 GHz, while the simulated peak gain is 7.2 dBi at the frequency 7.4 GHz.

The simulated radiation efficiency of the proposed DRA is higher than 90% across its entire bandwidth. The far-field radiation is measured in an anechoic chamber. Simulated and measured radiation patterns are plotted for $\Phi = 0^\circ$ and $\Phi = 90^\circ$ planes for resonant frequencies of 6 GHz and 7.5 GHz, as illustrated in Fig. 6(e) and Fig. 6(f), respectively. The DRA exhibits linear polarization and radiates in the broadside direction. It maintains a stable radiation pattern across the entire operating frequency range, consistent with the modes predicted by the proposed structure. The measured and simulated results of co-polarized radiation patterns at the $\Phi = 0^\circ$ and $\Phi = 90^\circ$ planes show excellent agreement. Both radiation patterns indicate that the proposed DRA exhibits low cross-polarization levels.

CBDRA = Conformal bent Dielectric Resonator Antenna, AC = Aperture Coupled, CSDRA = Conformal Stacked DRA, SFADRA = Slot Fed Arc-shaped DRA, RDRA = Rectangular DRA, CPP = Conformal Parasitic Patch, CMPA = Conformal Microstrip Patch Antenna, CPA = Conformal Patch Antenna, CPW = Co-Planar Waveguide, CRDRA = Conformal Rectangular DRA, IF = Integrated Feed, IB = Impedance Bandwidth, P.W. = Proposed work.

A comparison of the other reported conformal DRAs and the proposed DRA characteristics is listed in Table 1. As evident from the table, a 51.5% wide impedance bandwidth is offered by the proposed conformal DRA with a compact, low-profile design that realizes 7.2 dBi of peak gain within the impedance bandwidth. The proposed investigation is found to be novel compared to the state of art on low-profile conformal DRA.

6. CONCLUSION

This paper offers a comprehensive investigation of integrating low-profile Dielectric Resonator Antennas (DRAs) onto a concave conformal ground plane with an emphasis on wideband applications. This research contributes to the field of antenna design by addressing the challenge of space constraints, presenting a viable solution for applications where low-profile and conformal characteristics are essential. The radiation characteristics of the conformal DRAs are investigated and compared. It is determined that bent DRAs have several advantages such as a more flexible gain and wider bandwidth. To validate this research, a prototype of the proposed DRA operating in its $TE_{22\delta}$ and $TE_{23\delta}$ modes is designed and fabricated. It is very compact, in low profile of $0.1\lambda_g$ and yields a high gain of 6.8 dBi (measured) with stable radiation pattern over the operating frequency band from 5.2 GHz to 8.8 GHz frequencies.

ACKNOWLEDGEMENT

The research described in this paper was supported by the SERB, DST project No. — CRG/2020/000635.

REFERENCES

[1] Petosa, A. and A. Ittipiboon, "Dielectric resonator antennas: A historical review and the current state of the art," *IEEE Antennas and Propagation Magazine*, Vol. 52, No. 5, 91–116, Oct. 2010.

[2] Mukherjee, B., P. Patel, and J. Mukherjee, "A review of the recent advances in dielectric resonator antennas," *Journal of Electromagnetic Waves and Applications*, Vol. 34, No. 9, 1095–1158, 2020.

[3] Esselle, K. P., "A low-profile rectangular dielectric-resonator antenna," *IEEE Transactions on Antennas and Propagation*, Vol. 44, No. 9, 1296–1297, Sep. 1996.

[4] Ryu, K. S. and A. A. Kishk, "UWB dielectric resonator antenna having consistent omnidirectional pattern and low cross-polarization characteristics," *IEEE Transactions on Antennas and Propagation*, Vol. 59, No. 4, 1403–1408, Apr. 2011.

[5] Gao, Y., Z. Feng, and L. Zhang, "Compact asymmetrical T-shaped dielectric resonator antenna for broadband applications," *IEEE Transactions on Antennas and Propagation*, Vol. 60, No. 3, 1611–1615, Mar. 2012.

[6] Sharma, A., A. Sarkar, A. Biswas, and M. J. Akhtar, "A-shaped wideband dielectric resonator antenna for wireless communication systems and its MIMO implementation," *International Journal of RF and Microwave Computer-Aided Engineering*, Vol. 28, No. 8, e21402, 2018.

[7] Maity, S. and B. Gupta, "Experimental investigations on wideband triangular dielectric resonator antenna," *IEEE Transactions on Antennas and Propagation*, Vol. 64, No. 12, 5483–5486, Dec. 2016.

[8] Chauhan, M., A. K. Pandey, and B. Mukherjee, "A novel compact cylindrical dielectric resonator antenna for wireless sensor network application," *IEEE Sensors Letters*, Vol. 2, No. 2, 1–4, Jun. 2018.

[9] Gupta, P. K., A. Rajput, M. Mishra, and B. Mukherjee, "A compact low profile, wideband and high gain stacked dielectric resonator antenna," *Electromagnetics*, Vol. 43, No. 3, 163–174, 2023.

[10] Gaonkar, A., M. Ayyappan, and P. Patel, "A novel fractal RDRA for C-band applications," *IEEE Transactions on Components, Packaging and Manufacturing Technology*, Vol. 13, No. 7, 995–1002, Jul. 2023.

[11] Mukherjee, B., P. Patel, and J. Mukherjee, "Hemispherical dielectric resonator antenna based on apollonian gasket of circles — A fractal approach," *IEEE Transactions on Antennas and Propagation*, Vol. 62, No. 1, 40–47, Jan. 2014.

[12] Gangwar, R. K., S. Singh, and D. Kumar, "A modified fractal rectangular curve dielectric resonator antenna for WiMAX application," *Progress In Electromagnetics Research C*, Vol. 12, 37–51, 2010.

[13] Kiran, D. V., D. Sankaranarayanan, and B. Mukherjee, "Compact embedded dual-element rectangular dielectric resonator antenna combining Sierpinski and Minkowski fractals," *IEEE Transactions on Components, Packaging and Manufacturing Technology*, Vol. 7, No. 5, 786–791, May 2017.

[14] Khalily, M., M. K. A. Rahim, and A. A. Kishk, "Bandwidth enhancement and radiation characteristics improvement of rectangular dielectric resonator antenna," *IEEE Antennas and Wireless Propagation Letters*, Vol. 10, 393–395, 2011.

[15] Gaonkar, A. and P. Patel, "Compact half H-shaped dielectric resonator antenna for wideband applications," *Microwave and Optical Technology Letters*, Vol. 64, No. 10, 1849–1857, 2022.

[16] Braaten, B. D., S. Roy, I. Irfanullah, S. Nariyal, and D. E. Anagnostou, "Phase-compensated conformal antennas for changing spherical surfaces," *IEEE Transactions on Antennas and Propagation*, Vol. 62, No. 4, 1880–1887, Apr. 2014.

[17] Liu, Y., H. Yang, Z. Jin, F. Zhao, and J. Zhu, "A multibeam cylindrically conformal slot array antenna based on a modified Rotman lens," *IEEE Transactions on Antennas and Propagation*, Vol. 66, No. 7, 3441–3452, Jul. 2018.

[18] Leung, K. W., "Conformal strip excitation of dielectric resonator antenna," *IEEE Transactions on Antennas and Propagation*, Vol. 48, No. 6, 961–967, Jun. 2000.

[19] Boyuan, M., J. Pan, E. Wang, and Y. Luo, "Conformal bent dielectric resonator antennas with curving ground plane," *IEEE Transactions on Antennas and Propagation*, Vol. 67, No. 3, 1931–1936, Mar. 2019.

[20] Boyuan, M., J. Pan, E. Wang, and D. Yang, "Miniaturized conformal arc dielectric resonator antennas using dielectric and metallic loading," *IEEE Access*, Vol. 7, 139 518–139 525, 2019.

[21] Boyuan, M., J. Pan, E. Wang, and D. Yang, "Estimation and utilization of ground effects on conformal dielectric resonator antennas," *IEEE Access*, Vol. 7, 162 387–162 394, 2019.

[22] Maity, S. and B. Gupta, "Approximate theoretical investigations on isosceles triangular dielectric resonator antennas and experimental validation," *IEEE Transactions on Antennas and Propagation*, Vol. 66, No. 5, 2640–2643, May 2018.

[23] Chowdhury, R. and R. K. Chaudhary, "Investigation on different forms of circular sectored-dielectric resonator antenna for improvement in circular polarization performance," *IEEE Transactions on Antennas and Propagation*, Vol. 66, No. 10, 5596–5601, Oct. 2018.

[24] Iqbal, J., U. Illahi, M. I. Sulaiman, M. M. Alam, M. M. Su'ud, M. N. M. Yasin, and M. H. Jamaluddin, "Bandwidth enhancement and generation of CP by using parasitic patch on rectangular DRA for wireless applications," *IEEE Access*, Vol. 7, 94 365–94 372, 2019.

[25] Boyuan, M., J. Pan, D. Yang, and Y.-X. Guo, "Investigation on homogenization of flat and conformal stacked dielectric resonator antennas," *IEEE Transactions on Antennas and Propagation*, Vol. 70, No. 2, 1482–1487, 2022.

[26] Monica, J. and P. Jothilakshmi, "A design of bandwidth-enhanced conformal antenna for aircraft applications," *IETE Journal of Research*, Vol. 69, No. 1, 447–459, 2023.

[27] Ketavath, K. N., D. Gopi, and S. S. Rani, "In-vitro test of miniaturized CPW-fed implantable conformal patch antenna at ISM band for biomedical applications," *IEEE Access*, Vol. 7, 43 547–43 554, 2019.